Talanta 119 (2014) 262–267

Contents lists available at ScienceDirect

Talanta

journal homepage: www.elsevier.com/locate/talanta

Development of 1,1′-oxalyldiimidazole chemiluminescent biosensor using the combination of graphene oxide and hairpin aptamer and its application

Joonsuh Kwun [a,b,1], Soyong Yun [a,c,1], Lucienne Park [a,d], Ji Hoon Lee [a,*]

[a] Luminescent MD, LLC, Hagerstown, MD 21742, United States
[b] Thomas Jefferson High School for Science and Technology, Alexandria, VA 22312, United States
[c] McLean High School, McLean, VA 22101, United States
[d] Department of Biology, University of Maryland, College Park, MD 20742, United States

ARTICLE INFO

Article history:
Received 4 September 2013
Received in revised form
30 October 2013
Accepted 31 October 2013
Available online 11 November 2013

Keywords:
Hairpin DNA aptamer
Vibrio
Biosensor
1,1′-Oxalyldiimidazole chemiluminescence
Graphene oxide

ABSTRACT

Highly sensitive biosensor with 1,1′-oxalyldiimidazole chemiluminescence (ODI-CL) detection was developed to rapidly quantify *Vibrio (V) parahaemolyticus* without time-consuming procedures such as multiple long-incubations and washings. When *V. parahaemolyticus* in Tris–HCl (pH 7) and hairpin DNA aptamer conjugated with TEX615 in DNA free deionized water were consecutively added in PBS buffer (pH 7.4) containing graphene oxides (GOs), *V. parahaemolyticus* and GOs bind competitively to hairpin DNA aptamer conjugated with TEX615 during 10 min of incubation at room temperature. Brightness of light immediately emitted with the addition of ODI-CL reagents (*e.g.*, ODI, H_2O_2) after the incubation was dependent on the concentration of *V. parahaemolyticus* in a sample. The dynamic range of linear calibration curve for the quantification of *V. parahaemolyticus* in a sample was from 4375 to 70,000 cells/ml. The limit of detection (LOD = background + 3 × standard deviation, 2230 cells/ml) of the biosensor operated with good accuracy, precision, and recovery was lower than those of conventional assay methods such as time-consuming and expensive enzyme-linked immunosorbent assays.

1. Introduction

Vibrio (V.) parahaemolyticus, a curved, rod-shaped, and Gram-negative bacterium, is known as a food-borne pathogen with *V. cholerae* and *V. vulnificus*. The infection of *V. parahaemolyticus* can usually occur when eating raw and undercooked seafood, drinking contaminant water, and transmitting *via*. fecal–oral route [1–3]. Unfortunately, the mechanism of diseases occurring with the infection of *V. parahaemolyticus* has not been completely elucidated [2,3]. Therefore, it is necessary for the development of highly sensitive analytical method capable of rapidly monitoring trace levels of *V. parahaemolyticus* in seafood and water to prevent infections such as acute gastroenteritis.

Enzyme-linked immunosorbent assays (ELISAs) are widely applied to quantify trace levels of *V. parahaemolyticus* [4–6]. Recently, polymerase chain reaction (PCR)—ELISA was developed to analyze *V. parahaemolyticus* in shellfish [7]. However, ELISAs using expensive and intractable antibodies, produced with the sacrifice of little animals, are complicated and time-consuming. In order to solve the critical disadvantages of ELISAs, Duan and coworkers developed cost-effective and tractable hairpin DNA aptamers, capable of rapidly binding *V. parahaemolyticus*, generated by SELEX (systematic evolution of ligands by exponential enrichment) [8]. They reported that the range of binding dissociation constants (Kd) for hairpin DNA aptamers was 16.88 to 24.03 nM. However, aptasensor using hairpin DNA aptamers has never yet been developed for the quantification of *V. parahaemolyticus* in a sample.

Recently, several research groups reported that single strand DNAs (ssDNAs) are immobilized on the surface of nanoparticles such as various types of carbon nanotubes (*e.g.*, single-, double-, and multi-walled carbon nanotubes) and graphene oxide and microfibers based on the principle of π–π stacking interaction between ssDNAs and micro- or nano-particles [9–15]. Also, fluorescent ssDNA (*i.e.*, ssDNA conjugated with fluorescent dye) bound with micro- or nano-particles cannot emit fluorescence due to the fluorescence resonance energy transfer (FRET) from fluorescent ssDNA to micro- or nano-particles [9–12]. In addition, fluorescent ssDNA immobilized on the surface of micro- or nano-particles cannot emit light in 1,1′-oxalyldiimidazole chemiluminescence (ODI-CL reaction) reaction because fluorescent ssDNAs excited by

* Corresponding author. Tel.: +1 301 393 9091.
E-mail address: jhlee@luminescentmd.com (J.H. Lee).
[1] These authors contributed equally in this research.

0039-9140/$ - see front matter © 2013 Elsevier B.V. All rights reserved.
http://dx.doi.org/10.1016/j.talanta.2013.10.067

chemically initiated electron exchange luminescence (CIEEL) mechanism of ODI-CL reaction [16–19] transfer energy to micro- or nano-particles based on the principle of chemiluminescence resonance energy transfer (CRET) [13,15].

Using the principles of FRET and CRET observed in fluorescent ssDNA bound with micro- or nano-particles, various guanine (G)-quadruplex aptasensors were developed for the quantifications of several target molecules (*e.g.*, ATP, thrombin, ochratoxin A) using G-rich ssDNA aptamers [9,10,12–14]. G-rich ssDNA aptamers transform to G-quadruplex DNAs when they bind with target molecules. G-quadruplex DNA bound with target molecule does not interact with micro- or nano-particles whereas G-rich ssDNA aptamers are immobilized on the surface of micro- or nano-particles. Based on the different physical properties of G-rich ssDNA aptamer and G-quadruplex DNA in the presence of micro- or nano-particles, fluorescent G-quadruplex DNA bound with target molecules emit fluorescence or ODI-CL, whereas fluorescent G-rich ssDNA patamer immobilized on the surface of micro- or nano-particles cannot emit fluorescence or ODI-CL due to the principles of FRET or CRET. G-quadruplex aptasensor with ODI-CL detection was faster and more sensitive than that with fluorescence detection because the background of former is much lower than that of latter [13]. Also, highly sensitive and simple hybridization methods with fluorescence or ODI-CL detection were developed based on the principles of FRET and CRET between fluorescent complementary probe (*i.e.*, complementary probe conjugated with fluorescent dye) and micro- or nano-particles [11,15]. Double strand DNAs (dsDNAs) formed from the hybridization between fluorescent complementary probe and target ssDNA do not interact with micro- or nano-particles, whereas complementary probes remaining after the hybridization are immobilized on the surface of micro- or nano-particles.

Duan and coworker reported that the region of hairpin DNA aptamer sequence, which is not G-quandruplex DNA aptamer, is responsible for the high-affinity binding to the surface of *V. parahaemolyticus* [8]. Hu and coworkers confirmed that fluorescent hairpin DNAs (*i.e.*, hairpin DNAs conjugated with fluorescent dye) immobilized on the surface of micro- or nano-particles do not emit fluorescence [20]. Research results observed by two research groups imply that an aptasensor with ODI-CL detection capable of quantifying *V. parahaemolyticus* in a sample can be developed using non-G-quadruplex DNA aptamers if fluorescent hairpin DNA aptamers bound to the surface of *V. parahaemolyticus* emit strong light without the photochemical interference (*e.g.*, quenching effect) of micro- or nanoparticles while fluorescent hairpin DNA aptamers immobilized on the surface of micro- or nano-particles do not emit light due to the principle of CRET. Based on the hypothesis, in this research, we developed for the first time a cost-effective aptasensor with ODI-CL detection capable of rapidly and simply quantifying *V. parahaemolyticus*. Detailed description about the chemiluminescent apatsensor using non-G-quadruplex aptamers and nanoparticles is below.

2. Experimental

2.1. Chemicals and materials

Heat-killed Vibrio positive control containg *V. parahaemolyticus*, *V. cholerae* and *V. vulnificus* was purchased from KPL (Gaithersburg, MD, USA). Cell numbers of each vibrio in dextran solution was evenly 2.2×10^7 cells/ml. Hairpin DNA aptamer [8] conjugated with TEX615 (5′–TEX615-TCT AAA AAT GGG CAA AGA AAC AGT GAC TCG TTG AGA TAC T-3′) was purchased from Integrated DNA Technologies (Coralville, Iowa, USA). We selected TEX615 as a fluorescent dye labeled with hairpin DNA aptamer because ODI-CL efficiency of TEX615 is better than those of other fluorescent dyes (*e.g.*, fluorescein, Texas Red) widely used for fluorescence and conventional peroxyoxalate chemiuminescence detection [13]. Graphene oxide (GO, 300–700 nm, 5 mg/ml, https://graphene-supermarket.com/Single-Layer-Graphene-Oxide-Dispersion-in-Water.html) dispersed in water was purchased from Graphene Supermarket (Calverton, NY, USA). Multi-walled carbon-nanotubes (20–30 nm) was purchased from Nanomaterial store (Fremont, CA, USA). Bis-2,4,6-trichloriphenyl oxalate (TCPO) and 4-methylimidazole (4MImH) were purchased from TCI, America (Portland, OR, USA). 30% H_2O_2 was purchased from VWR (Philadelphia, PA, USA). Rhodamine 101 and EDTA were purchased form Sigma-Aldrich (Allentown, PA, USA). DNA free deionized water, HPLC grade ethyl acetate, and isopropyl alcohol were purchased from EMD (Billerica, MA, USA). PBS and Tris–HCl buffers were purchased from Polysciences, Inc (Warrington, PA, USA).

2.2. Procedures

2.2.1. Effect of nanoparticles in ODI-CL reaction

In this research, 20 nM Rhodamine 101 was prepared in water instead of TEX615 used as a fluorescent dye conjugated with hairpin DNA aptamer. This is because pure TEX615 is not available commercially, and Rhodamine 101 emits bright light in ODI-CL reaction shown in Scheme 1. 5 different concentrations (0.06, 0.13, 0.25, 0.5, and 1 mg/ml) of GO and MWCNT were prepared in water. ODI was synthesized from the reaction of 5 μM TCPO and 20 μM 4MImH in ethyl acetate. 0.2 M H_2O_2 was prepared in isopropyl alcohol. In order to study photochemical and photophysical properties of GO and MWCNT in ODI-CL reaction, rhodamine 101 (50 μl) and GO or MWCNT (50 μl) was mixed in a 0.5-ml microcentrifuge tube. The mixture (10 μl) was poured into a borosilicate test tube (12×75 mm^2, VWR). The tube was inserted into a sample holder of Lumat 9507 with two dispensers (Berthold Inc., Germany). When the start button was pressed, H_2O_2 (25 μl) was injected into the test tube through the first dispenser. Then, light emitted in the test tube was immediately measured for 1 s with the addition of ODI (25 μl) through the second dispenser.

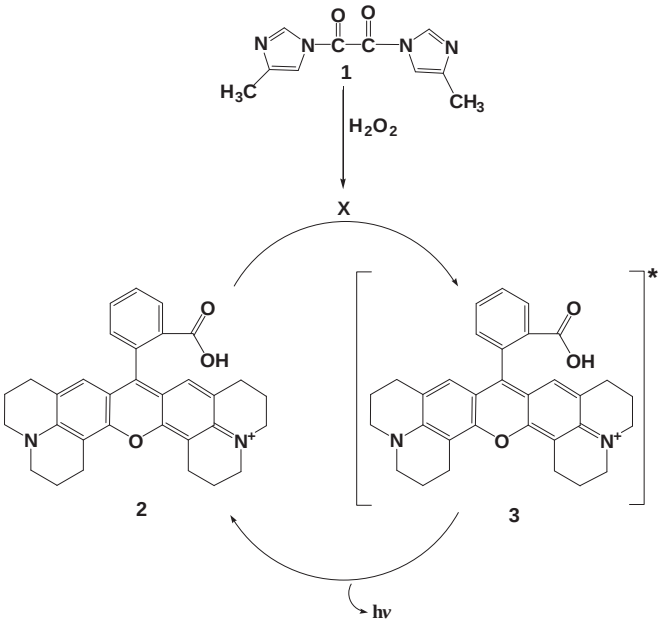

Scheme 1. ODI-CL reaction in the presence of Rhodamine 101. **1** 1,1′-Oxalyldi-4-methy-imidazole, **2** Rhodamine 101 under the ground state, **3** Rhodamine 101 under the excited state, **X** high-energy intermediate capable of transferring energy to rhodamine 101.

2.2.2. Selection of buffer solution

Four different pH TE buffers (pH 7, 7.5, 8, and 8.5) containing 5 mM EDTA and 10 mM Tris–HCl were prepared. PBS buffer (pH 7.4, components: 137 mM NaCl, 2.7 mM KCl, and 10 mM phosphate buffer) purchased from EMD was 10-fold diluted in water. 110 μg/ml GO was added in each buffer. Hairpin DNA aptamer conjugated with TEX615 (10 μM) was dissolved in water to use as a stock solution. Then, 200 nM hairpin DNA aptamer conjugated with TEX615 (1 ml) was prepared as a working solution in a 1.5-ml microcentrifuge tube. The working solution (100 μl) was mixed with GO (100 μl) in each PBS buffer. The mixture was incubated for 10 min at room temperature. Light emitted from the mixture in ODI-CL reaction was measured with Lumat 9507 through the same procedures described in Section 2.2.1.

2.2.3. Quantification of V. parahaemolyticus

In order to develop a biosensor capable of sensing *V. parahaemolyticus* in a sample, the stock solution (2.2×10^7 cells/ml) of *V. parahaemolyticus* was prepared in Luria Bertani (LB) broth (components: 1.0% tryptone, 0.5% yeast extract, 1.0% NaCl, pH 7.5). Each stock solution (20 μl) aliquoted in 0.5-ml microcentrifuge tube was stored at an ultra-low freezer (−80 °C, So-Low). Working solutions (*e.g.*, standards, samples) containing a certain concentration of *V. parahaemolyticus* was prepared with the dilution of stock solution using Tris–HCl (pH 7). GO (110 μg/ml) was prepared in PBS buffer (pH 7.4) containing 1 mM phosphate buffer, 13.7 mM NaCl, and 0.27 mM KCl. 200 nM hairpin DNA aptamer capable of capturing *V. parahaemolyticus* was prepared in DNA free deionized water. ODI synthesized from the reaction of TCPO (5 μM) and 4MImH (20 μM) in ethyl acetate and H_2O_2 (0.2 M) in isopropyl alcohol were used as ODI-CL reagents. Hairpin DNA aptamer (100 μl) was added in a 1.5-ml microcentrifuge tube containing standard or sample (100 μl). After the 10-minute incubation of the mixture in a Thermomixer R (Eppendorf, Inc.) at 37 °C, GO (200 μl) was added in the 1.5-ml microcentrifuge tube. Then, the final mixture was rapidly mixed with a vortex mixer (VWR) for one second. Finally, light emitted from the complex of *V. parahaemolyticus* and hairpin DNA aptamer-conjugated TEX615 in each mixture was measured using Lumat 9507 with two dispensers as described in Section 2.2.1.

3. Results and discussion

3.1. Effect of nanoparticles in ODI-CL reaction

As shown in Fig. 1, MWCNT acts as a quencher in ODI-CL reaction. Recently, Kim et al. reported that MWCNT is a static quencher in ODI-CL reaction because Rhodamine 101 adsorbed on the surface of MWCNT cannot emit light due to CRET between Rhodamine 101 and MWCNT [21]. As proof, they observed that the time (τ_{max}) necessary for attaining maximum CL intensity (I_{max}) as well as the time (τ_{half}) necessary for decaying up to $1/e$ of I_{max} in the absence of Rhodamine 101was the same as those in the presence of Rhodamine 101 even though I_{max} of the former is higher than that of the latter [21].

However, Fig. 1 indicates that GO does not act as a chemical and physical interference in the emission of Rhodamine 101 in ODI-CL reaction. Also, we confirmed that τ_{max} (0.5 s) and τ_{half} (1.5 s) do not depend on the concentration of GO. Thus, GO does not act as a static as well as dynamic quencher in ODI-CL reaction.

The results shown in Fig. 1 indicate that an aptasensor with ODI-CL detection using GO capable of quantifying *V. parahaemolyticus* in a sample is more sensitive than that using MWCNT.

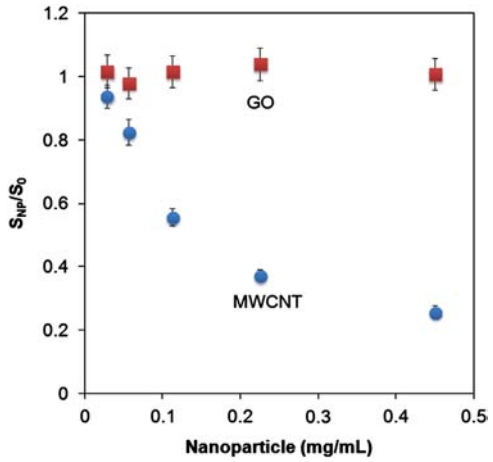

Fig. 1. Effect of GO and MWCNT in ODI-CL reaction. Each value was obtained in triplicate experiments.

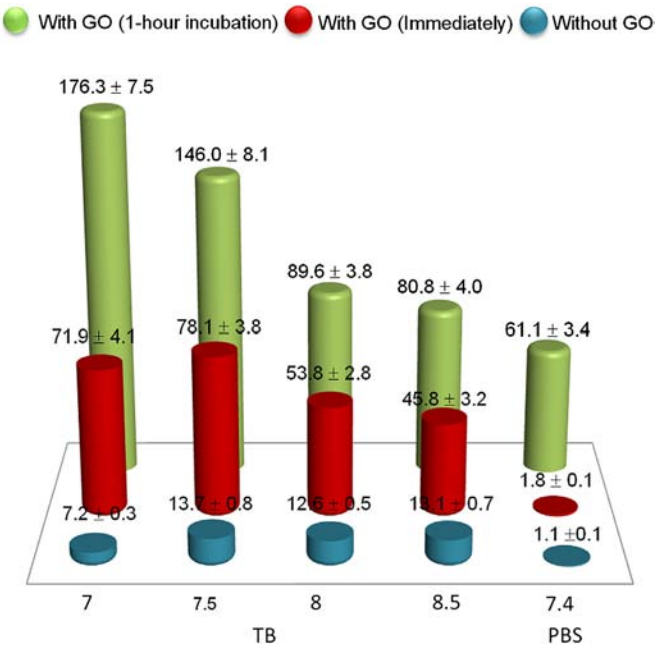

Fig. 2. Effect of buffer solution to immobilize hairpin DNA aptamer-conjugated TEX615 on the surface of GO. The error range of values measured under various experimental conditions was 3–6%. Each value was obtained in triplicate experiments.

3.2. Selection of buffer

Fig. 2 shows that π–π interaction between haripin DNA aptamer-conjugated TEX615 and GO is dependent on the type of buffer as well as pH of TE buffer prepared with 10 mM Tris–HCl buffer and 5 mM EDTA.

The signal to background ratio of hairpin DNA aptamer-conjugated TEX615 in TE buffer (pH 7) is higher than those in the rest of the TE buffers and PBS buffer (pH 7.4) because light emitted in ODI-CL reaction at neutral pH condition is brighter than that at basic pH condition [22].

Signal immediately measured with the addition of GO in PBS buffer containing hairpin DNA aptamer-conjugated TEX615 was similar to background measured in the presence of only GO. It indicates that hairpin DNA aptamers are rapidly immobilized on the surface of graphene oxide in PBS buffer. The result implies that hairpin DNA aptamer-conjugated TEX615 is rapidly immobilized on the surface of GO in the presence of alkali metals (*e.g.*, Na^+ and

K^+). Signal to background ratio after the 1-hour incubation of the mixture didn't change within the acceptable error range (5%, $n=3$). It indicates that hairpin DNA aptamer immobilized on the surface of GO is stable.

The immobilization of hairpin DNA aptamer on the surface of GO was dependent on pH of TE buffer. Fig. 2 indicates that π–π interaction between hairpin DNA aptamer-conjugated TEX615 and GO in pH 7 is faster than those in the rest of the buffers. Thus, signal to background ratio immediately determined with the addition of GO in TE (pH 7) containing hairpin DNA aptamer-conjugated TEX615 was smaller than that in TE (pH 7.5) even though signal to background ratio of the former in the absence of GO was higher than that of the latter in the absence of GO. Reduction rate of signal to background ratio in the presence of GO at pH 7 was larger than those at the rest of the pH ranges. Thus, signal to background ratio after the 1-h incubation of mixture in TE (pH 7) was the lowest. However, signal to background ratio calculated in this condition was still higher than that immediately measured with the addition of GO in PBS buffer containing hairpin DNA aptamer-conjugated TEX615.

In order to develop highly sensitive aptasensor, based on the results shown in Fig. 2, we selected PBS buffer capable of rapidly and stably immobilizing hairpin DNA aptamer-conjugated TEX615 on the surface of GO.

3.3. Possible mechanism for the quantification of V. parahemolyticus using hairpin DNA aptamer-conjugated TEX615 and GO

As shown in Fig. 3, it is possible to quantify *V. parahaemolyticus* using two different mechanisms. Fig. 3(a) shows that hairpin DNA aptamers immobilized on the surface of GO interact with *V. parahaemolyticus* before adding ODI-CL reagents to measure light emitted from the complex of *V. parahaemolyticus* and hairpin DNA aptamers come from the surface of GO. As the other mechanism shown in Fig. 3(b), *V. parahaemolyticus* and hairpin DNA aptamer can simultaneously (or consecutively) added in the solution containing GO. The complex of *V. parahaemolyticus* and hairpin DNA aptamer form competitively with the immobilization of hairpin DNA aptamer on the surface of GO for a certain period of incubation before adding ODI-CL reagents.

Fig. 4 shows that signal to background ratios using b mechanism of Fig. 3(b) was higher than those using a mechanism of Fig. 3(a). The results of Fig. 4 indicate that b mechanism for the quantification of *V. parahaemolyticus* is more sensitive than a mechanism. Also, the time necessary for the analysis of *V. parahaemolyticus* in a sample using the former is faster than that using the latter. Thus, we selected b mechanism of Fig. 3 to develop a new biosensor capable of sensing trace levels of *V. parahaemolyticus* in a sample.

3.4. Determination of incubation time between V. parahaemolyticus and hairpin DNA aptamer-conjugated TEX615

In order to develop a biosensor based on the mechanism shown in Fig. 3(b), *V. parahaemolyticus* (20,000 cells/ml in Tris–HCl buffer at pH 7) and hairpin DNA aptamer-conjugated TEX615 (200 nM in DNA free deionized water) were consecutively added in PBS buffer containing GO (110 μg/ml). The mixture was incubated for three different time periods (*e.g.*, 10, 30, 60 min) as shown in Fig. 5. Relative CL intensity after the 10-min incubation was the same as those after the 30-min and 60-min incubations within a statistically acceptable error range (5%, $n=3$). As shown in Fig. 5, signal in the presence of *V. parahaemolyticus* (20,000 cells/ml) was about 3.3 times higher than background in the absence of *V.*

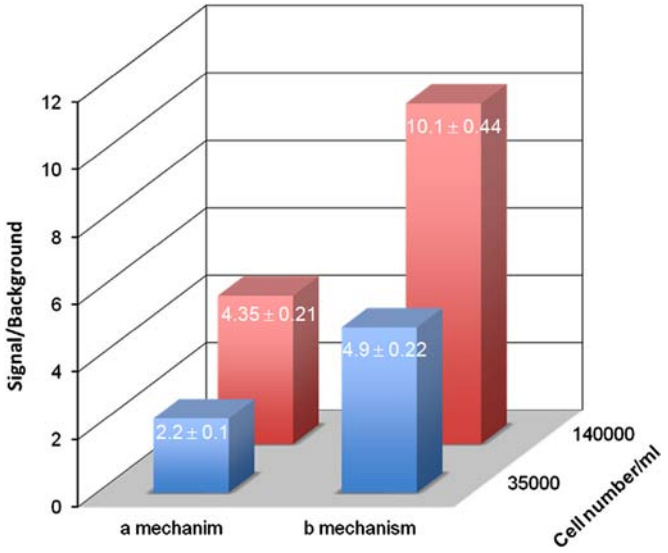

Fig. 4. Efficiency of biosensor with ODI-CL detection through (a) and (b) mechanisms. Each value was obtained in triplicate experiments.

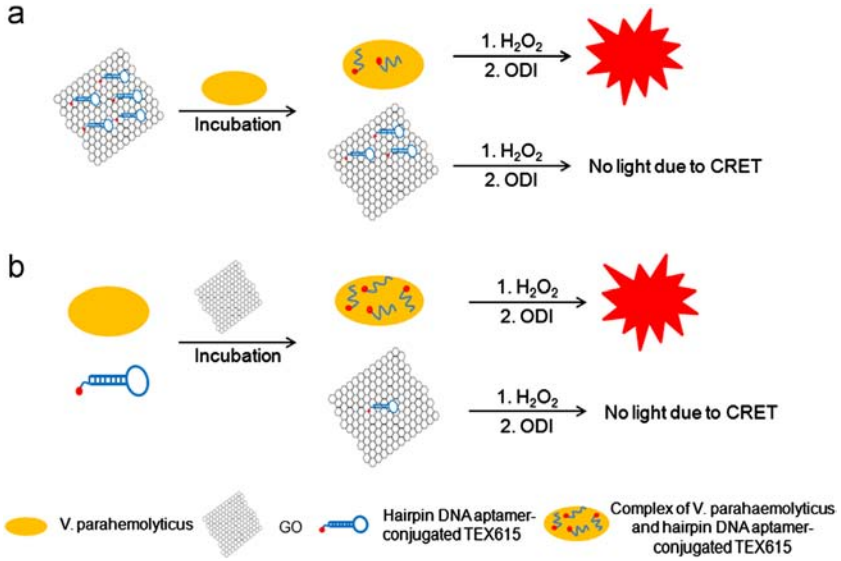

Fig. 3. Possible mechanisms for quantifying *Vibrio parahaemolyticus* using biosensor with ODI-CL detection.

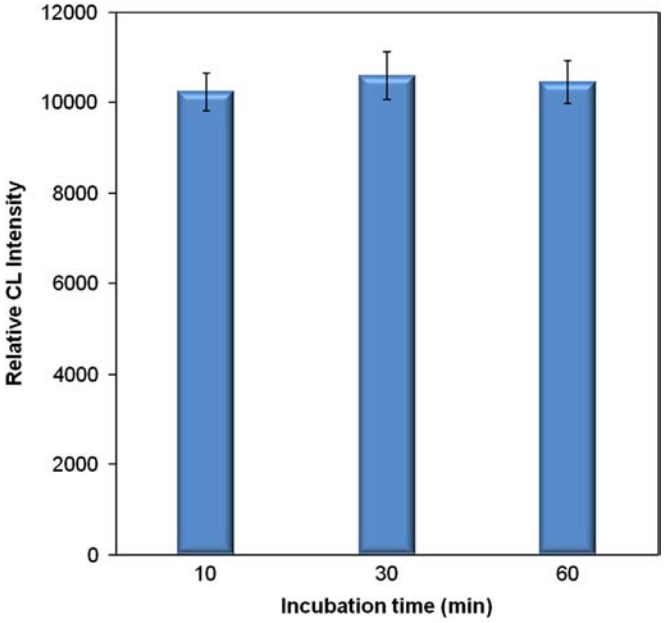

Fig. 5. Effect of incubation time for the quantification of *V. parahaemolyticus* (20,000 cells/ml) using biosensor with ODI-CL detection. Each value was obtained in triplicate experiments.

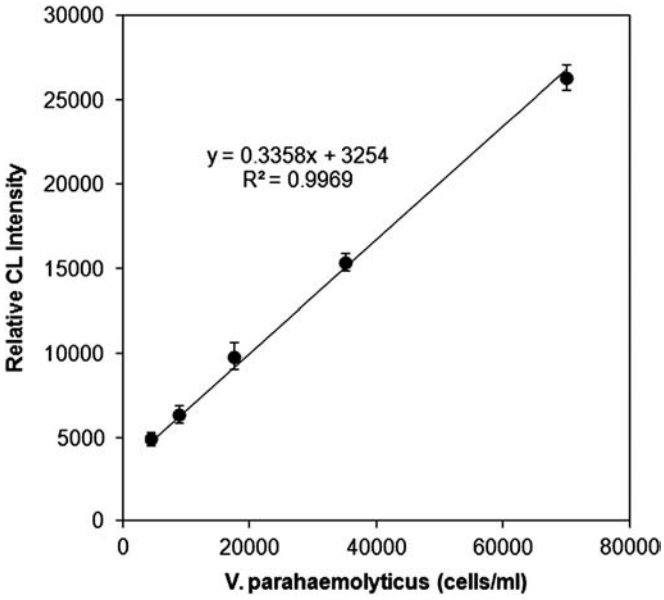

Fig. 6. Calibration curve for the quantification of *V. parahaemolyticus* using biosensor with ODI-CL detection. Each value was obtained in triplicate experiments.

parahaemolyticus. The results of Fig. 5 imply that biosensor capable of rapidly detecting trace levels of *V. parahaemolyticus* might be more sensitive than conventional immunoassays such as ELISAs.

3.5. Quantification of V. parahaemolyticus using a new biosensor

We were able to rapidly quantify trace levels of *V. parahaemolyticus* with the linear calibration curve (see Fig. 6) obtained using the highly sensitive biosensor developed based on the preliminary experimental data described above. The dynamic range of linear calibration curve was from 4375 to 70,000 cells/ml. The limit of detection (LOD = background + 3 × standard deviation) [13,21,24] of the biosensor was 2230 cells/ml. As shown in Table 1, rapid biosensor developed in this research was more sensitive than conventional immunoassays. Also, the biosensor was much faster than all the other analytical methods shown in Table 1. Table 2 demonstrates that accuracy and precision of biosensor determined using the calibration curve of Fig. 6 were good. Also, the recovery of biosensor determined using mixture of two samples was good within statistically acceptable error range.

Table 1
Comparison between new biosensor and conventional methods to quantify *Vibrio parahaemolyticus* in a sample.

Method	Detector	Incubation time (min)	LOD (cells/ml)	Reference
Hairpin DNA aptasensor	ODI-CL	10	2,230	This research
Sandwich ELISA	Colorimeter	250	25,000	[4]
ELISA-On-A-Chip	Colorimeter	20	620,000	[5]
Enzyme immunsensor	Amperometric	>600	73,740	[6]
Immunochromatography	Naked eye	<15	100,000	[23]

Table 2
Accuracy, precision, and recovery of biosensor ($n=3$).

Sample 1[a]	Sample 2[a]	Calculated [a,b]	Measured [a,c]	Accuracy (%)	Precision (%)	Recovery (%)
8,750	140,000	74,375	69,224	6.9	6.1	93.1
17,500	70,000	43,750	44,288	3.5	5.2	103.5
35,000	70,000	52,500	50,183	4.4	3.7	95.6

[a] cell/ml of *V. Parahaemolyticus*.
[b] Calculated value = (sample 1 + sample 2)/2.
[c] Measured values in the mixture of sample 1 and sample were determined with the calibration curve shown in Fig. 6.

4. Conclusions

In summary, we confirmed for the first time that hairpin DNA aptamer, which is a non-quadruplex DNA aptamer, can rapidly bind to GO in PBS buffer (pH 7.4). Also, hairpin DNA aptamer-conjugated TEX615 immobilized on the surface of GO cannot emit ODI-CL due to CRET from excited hairpin DNA aptamer-conjugated TEX615 to GO. Based on these phenomena, we developed a highly sensitive biosensor capable of rapidly quantifying *V. parahaemolyticus* in a sample. Thus, we expect that the biosensor with ODI-CL detection reported in this paper can be applied to rapidly quantify various food-borne pathogens (*e.g., Escherichia coli, Salmonella, Listeria*) with excellent accuracy and precision. Previous report related to ODI-CL reaction [24] indicates that color emitted from the biosensor with ODI-CL detection is dependent on properties of fluorescent dye labeled with DNA aptamer. In other words, it is possible to develop a biosensor capable of simultaneously detecting multiple colors emitted from DNA aptamers conjugated with various fluorescent dyes. Various DNA aptamers to analyze a specific food-borne pathogen have been developed. Thus, in the future, we expect that an ODI chemiluminescent biosensor using multiple specific-DNA aptamers conjugated with different fluorescent dyes can be developed to simultaneously quantify multiple food-borne pathogens in a sample.

Acknowledgements

This research was performed based on the intern program (LST-2012-08) of Luminescent MD, LLC.

References

[1] C.A. Broberg, R.J. Calder, K. Orth, Microbes. Infect. 13 (2011) 992–1001.
[2] S. Shinoda, Biocontrol Sci. 16 (2011) 129–137.
[3] L.L. Zhang, K. Orth, Curr. Opin. Microbiol. 16 (2013) 70–77.
[4] Q.P. Zhong, Y.Q. Dong, L. Wang, B.B. He, Development of IgY-based sandwich enzyme-linked immunosorbent assay for the detection of *Vibrio parahaemolyticus*, in: E. Zhu, S. Sambath (Eds.), Information Technology and Agricultural Engineering, vol. 134, Springer-Verlag, Berlin Heidelberg, New York, 2012, pp. 517–524.
[5] S.-M. Seo, I.-H. Cho, J.-W. Jeon, H.-K. Cho, E.-G. Oh, H.-S. Yu, S.-B. Shin, H.-J. Lee, S.-H. Paek, J. Food Protect. 73 (2010) 1466–1473.
[6] G.Y. Zhao, F.F. Xing, S.P. Deng, Electrochem. Commun. 9 (2007) 1263–1268.
[7] A.D. Pinto, V. Terio, P.D. Pinto, V. Colao, G. Tantillo, Lett. Appl. Microbiol. 54 (2012) 494–498.
[8] N. Duan, S.J. Wu, X.J. Chen, Y.K. Huang, Z.P. Wang, J. Agric. Food Chem. 60 (2012) 4034–4038.
[9] L.F. Sheng, J.T. Ren, Y.Q. Miao, J.H. Wang, E.K. Wang, Biosens. Bioelectron. 26 (2011) 3494–3499.
[10] Z.J. Guo, J.T. Ren, J.H. Wang, E.K. Wang, Talanta 85 (2011) 2517. (521).
[11] H. Li, X. Sun, Anal. Chim. Acta. 702 (2011) 109–113.
[12] C. Yang, Y. Wang, J.-L. Marty, X. Yang, Biosens. Bioelectron. 26 (2011) 2724–2727.
[13] L. Park, J. Kim, J.H. Lee, Talanta 116 (2013) 736–742.
[14] W.D. Pu, L. Zhang, C.Z. Huang, Anal. Methods 4 (2012) 1662–1666.
[15] W. Choi, J.H. Choi, J.H. Lee, RSC Adv. 3 (2013) 22455–22460.
[16] J.H. Lee, J.C. Rock, S.B. Park, M.A. Schlautman, E.R. Carraway, J. Chem. Soc. Perk. Trans 2 (2002) 802–809.
[17] J.H. Lee, J.C. Rock, M.A. Schlautman, E.R. Carraway, J. Chem. Soc. Perk. Trans 2 (2002) 1653–1657.
[18] T. Maruyama, S. Narita, J. Motoyoshiya, J. Photochem., Photobio. A-Chem 252 (2013) 222–231.
[19] P.S. Park, T.H.D. Rho, Y.T. Kim, S.O. Ko, M.A. Schlautman, E.R. Carraway, J.H. Lee, Chem. Commun. 47 (2011) 5542–5544.
[20] K. Hu, J. Liu, J. Chen, Y. Huang, S. Zhao, J. Tian, G. Zhang, Biosens. Bioelectron. 42 (2013) 598–602.
[21] J. Kim, L. Park, J. Kim, J. H. Lee, Lumin, submitted.
[22] J.H. Lee, J. Je, J. Hur, M.A. Schlautman, E.R. Carraway, Analyst 128 (2003) 1257–1261.
[23] A. Guo, H.L. Sheng, M. Zhang, R.W. Wu, J. Xie, J. Food Qual. 35 (2012) 366–371.
[24] R. Chong, J.E.R. Rho, H.J. Yoon, T.H.D. Rho, P.S. Park, Y.H. Kim, J.H. Lee, Biosens. Bioelectron. 32 (2012) 19–23.